Published July 18, 2019

Technical Notes

Core Ideas

- Specimen preparation methods have a significant influence on hydraulic conductivity.
- The difference caused by different methods can be large as one order of magnitude.
- Soil pore structure should be considered in predicting hydraulic conductivity.
- A pore-information-based model is presented to predict hydraulic conductivity.
- The new model is more accurate than traditional particle information based models.

Evaluating the Influence of Specimen Preparation on Saturated Hydraulic Conductivity Using Nuclear Magnetic Resonance Technology

Jidong Teng, Jingyuan Kou, Sheng Zhang,* and Daichao Sheng

A series of laboratory tests were performed to investigate the influences of specimen preparation on pore size distribution of soil and saturated hydraulic conductivity (K_s). Nuclear magnetic resonance technology was used to measure the pore size distribution of the saturated samples of silty soil, which were prepared by three different kinds of methods: Proctor compaction, static compaction, and the consolidation method. The K_s of the samples was measured by the falling head permeability test. The results show that the difference in K_s caused by different specimen preparations can be large as one order of magnitude, as the measured K_s varied from 3.09×10^{-3} to 3.36×10^{-4} cm s^{-1}. The consolidated specimen tended to have the greatest K_s value, followed by those prepared by Proctor compaction and static compaction. The observed difference highlights the importance of pore structure in determining K_s. This study also presents a pore-information-based theoretical approach for predicting K_s. A comparison of measured data shows that the proposed model performs better than the traditional void-ratio-based models.

Abbreviations: FID, free induction decay; K–C, Kozeny–Carman; NMR, nuclear magnetic resonance.

Saturated hydraulic conductivity (K_s) is a key physical variable of soil and is used to determine infiltration rate, percolation depth, and other hydrological processes (Malusis et al., 2003; Zhang et al., 2016; Jafari et al., 2017; Teng et al., 2019a). It has been revealed that K_s depends on several factors such as soil texture and structure, chemical properties of the fluid, and pore structure (Hillel, 1982; Boynton and Daniel, 1985; Costa, 2006; Jang et al., 2011). A number of studies have investigated the effects of different sampling procedures on the anisotropy of K_s, which is caused by the anisotropy of pore structure and the differences in the cross-section of water flow (Bathke and Cassel, 1991; Burger and Belitz, 1997; Surridge et al., 2005; Iwanek, 2008; Bagarello et al., 2009). It is noted that the measurement of K_s can be divided into in situ measurement and laboratory measurement. Some useful methods are widely applied to the in situ measurement of K_s—for example, the borehole measurements, tracer tests, and core sampling methods in combination with laboratory permeameter tests (Bouma and Dekker, 1981; Reynolds and Elrick, 1985; Amoozegar, 1989; Reeves et al., 1996; Beckwith et al., 2003; Germer and Braun, 2015). In the laboratory, K_s can be measured by a constant head permeability test or the falling head permeability test. It is noted that the measured K_s of the remolded soil is generally based on a compacted specimen. Such a compacted specimen is usually prepared by oven drying and sieving to dry soil powder, mixing with sprayed water to achieve a target initial gravimetric water content, and then static or dynamic compaction to a target dry unit weight. However, compacted specimens cannot represent the hydraulic properties of natural soil, particularly those consolidated from slurry deposits, or those residual soils from weathering (Reynolds 2008; Li and Zhang, 2009; Gao et al., 2016; Teng et al., 2016). The consolidated specimen is prepared by gradually increasing the loading pressure to an initially saturated soil until the soil volume reaches a target value. In these cases,

J. Teng, J. Kou, S. Zhang, and D. Sheng, National Engineering Lab. for High-Speed-Railway Construction, Central South Univ., Changsha 410075 China; D. Sheng, School of Civil and Environmental Engineering, Univ. of Technology Sydney, Sydney, NSW, Australia. *Corresponding author (zhang-sheng@csu.edu.cn).

Received 18 Sept. 2018.
Accepted 27 Jan. 2019.

Citation: Teng, J., J. Kou, S. Zhang, and D. Sheng. 2019. Evaluating the influence of specimen preparation on saturated hydraulic conductivity using nuclear magnetic resonance technology. Vadose Zone J. 18:180179. doi:10.2136/vzj2018.09.0179

a consolidated specimen may represent the properties of natural soils more accurately.

The specimen preparation method has an evident influence on the pore size distribution of the soil (Delage et al., 1996). It has been reported that two populations of soil pores, interaggregate pores and intra-aggregate pores, are formed during the compaction of fine-grained soils (Li and Zhang, 2009). The interaggregate pores, which are not as stable as the smaller intra-aggregate pores, can be removed by either wetting or applying large external loading (Tarantino and de Col, 2008; Tarantino, 2011; Sheng et al., 2014). Compared with compacted specimens, consolidated specimens tend to show a unimodal pore size distribution with a single population of soil pores (Gao et al., 2016). Considering that compaction is still the dominant sampling method in laboratory testing, questions are raised: for example, does specimen preparation influence K_s or not, and how do you quantitatively evaluate the difference if it exists?

An accurate and reliable prediction of K_s has been a long-standing topic of interest for geotechnical and geological researchers (Ren et al., 2016; Teng et al., 2019b). One of the most common models for K_s is the Kozeny–Carman equation (referred to as the K–C equation):

$$K_s = C_F\left(\frac{1}{S_S^2}\right)\left(\frac{\gamma_w}{\mu\rho_m^2}\right)\left(\frac{e^3}{1+e}\right) \quad [1]$$

The K–C equation shows that K_s (cm s^{-1} or m s^{-1}) is governed by void ratio e (unitless), soil density ρ_m (kg m^{-3}), specific surface area S_s, which is defined as the total surface area of soil particle per unit of mass (m^2 g^{-1}), and a dimensionless shape constant C_F if information on the fluid, such as the unit weight of the fluid γ_w (N m^{-3}) and fluid viscosity μ (m^2 s^{-1}) (Kozeny, 1927; Carman, 1937), is known. Predicted results of the K–C equation agree well with experimental results for coarse-grained soils such as sand, but less so for fine-grained soils, largely because this equation neglects the electrochemical reaction between the solid particles and fluid (Carrier, 2003). Following the approach of the K–C equation, many researchers have suggested alternative relations for a wider range of soils. These works either modify the definitions of the parameters, such as the void ratio and specific surface area, in the K–C equation, or introduce a new parameter, such as the plastic limit or the diameter D_{10} (10% of the particles is smaller than this diameter), to account for the effects of fine-grained particles (Taylor, 1948, p. 97–123; Wyllie et al., 1958; Carrier and Beckman, 1984; Dolinar, 2009; Indraratna et al., 2012; Kucza and Ilek, 2016; Ren and Santamarina, 2018). It is noted that most predictions of K_s in the literature are based on information of the solid particles instead of information of the soil pores. In theory, K_s depends more on the pore sizes and on how the pores are distributed and interconnected (Chapuis, 2012; Teng et al., 2014). A theoretical description of the complex pore structure of soil is needed to simulate K_s, although obtaining such a description may be challenging.

The objective of this study was to investigate the influence of specimen preparations on pore size distribution of soil and hence on K_s. The pore size distribution was measured by nuclear magnetic resonance (NMR) technology, which established a connection between the specimen preparations and K_s. In addition, a soil-pore-information-based mathematical model was developed to describe K_s.

Materials and Methods

Laboratory Measurement

The specimen used in the laboratory test was sampled at the depth of 2.0 m in an exploratory trench by cutting ring method. The sampling spot was close to the Zhongchuan Airport of Lanzhou City, China. The soil belonged to the Malan loess, which is composed of a kind of silty soil with low content of organic matter. The soil is a silty clay loam according to the International Soil Science Society (ISSS) classification, with 14% sand, 67% silt, and 19% clay, a specific gravity of 2.70 g cm^{-3}, liquid and plastic limits of 29.92 and 15.99%, an optimum moisture content of 17.00%, and maximum dry density of 1.80 g cm^{-3}. The D_{10} and D_{60} of the specimen were 3 and 42 μm, respectively. The oven-dried sample was first placed on a flat plate surface, and then a certain amount of distilled water was sprayed evenly on the soil surface. A layer of dry soil was sprinkled on the wet surface, and the above process was repeated. The soil was then stirred and placed in a plastic bag for 24 h to ensure that the moisture in the soil had distributed uniformly. Therefore, a soil with a controlled initial water content of 17.00% was prepared for either Proctor compaction testing or static compaction testing.

The Proctor compaction test was conducted according to the ASTM D1557 (ASTM, 2009) standard. The dry density of the specimen was determined by controlling the compaction effort. For the static load compaction, a certain amount of soil was packed into the Proctor mold in two layers. A constant rate of axial loading pressure was applied to the specimen until the target density was achieved (Venkatarama Reddy and Jagadish, 1993; Islam and Kodikara, 2016). When preparing the consolidated specimen, the sample was mixed with a certain amount of distilled water, resulting in a slurry sample at two times the liquid limit. The slurry sample was decanted into a steal cylinder, and the consolidation pressure was applied step by step until the target height of the specimen was achieved. The final water content of the consolidated specimen was ~26%. Notably, the state conditions (void ratio, stress path, etc.) were strictly controlled to be the same for specimens with different specimen preparation methods, to ensure the validity of the comparison.

Three dry densities (1.40, 1.60, and 1.80 g cm^{-3}) were evaluated for the specimens in the Proctor compaction and static compaction tests. Two dry densities (1.40 and 1.60 g cm^{-3}) were used in the consolidation test. For each density, four specimens were prepared: two of them were used to measure the pore size distribution, and the other two specimens were used in the permeability test. Parallel testing of two specimens was designed to reduce the error of the experiment.

The specimens used for the permeability tests were obtained by using a 61-mm-i.d. cutting tube (40 mm in height). The K_s was measured for each condition with a falling head method (ASTM D5084-10; ASTM, 2014). The pore size distribution of each specimen was measured twice by using the NMR technology. A photo of the NMR device is shown in Fig. 1. The NMR technology can evaluate the pore water content or pore size distribution by measuring the free induction decay (FID) curve. The T_2 relaxation times of protons in the porous medium can be obtained from the FID curve by applying the Fourier transformation. In water-saturated porous media, T_2 is linearly proportional to the pore size, such that the pore size distribution of the sample can be determined (Coates et al., 1999; Jaeger et al., 2009). It is noted that all the specimens were saturated under vacuum conditions before the permeability test and NMR test, to ensure that the conditions of soil pore structure during the two tests were consistent.

Prediction of Saturated Hydraulic Conductivity Based on Pore Size Distribution

In this section, a new model that takes into account the pore size distribution is introduced for predicting K_s. According to the capillary model, the pore channels in a soil are replaced by parallel capillary tubes (as shown in Fig. 2) (Deng et al., 2011; Ilek and Kucza, 2014). The ratio and the cross-sectional area of the capillary tubes are defined as R and a, respectively. The head loss is defined as h for a given length L, and the hydraulic gradient is $i = h/L$. The total seepage force of the tubular water body with radius r is $\pi r^2 \gamma_w h$, where γ_w is the unit weight of the soil. The surrounding water resistance is $2\pi rL\tau$, where τ is the water viscosity and is equal to $-\mu dv/dr$, with μ and v representing the dynamic viscosity coefficient and the flowing velocity, respectively.

We let the resistance equal the total seepage force, which can be expressed as

$$2\mu dv = \gamma_w i r dr \quad [2]$$

The flow velocity through radius r can be obtained by integrating Eq. [2] with the boundary conditions $r = R$ and $v = 0$:

$$v = \frac{\gamma_w i}{4\mu}\left(R^2 - r^2\right) \quad [3]$$

The flow through cross-section R is

$$Q = \int_0^R v 2\pi r dr \quad [4]$$

Substituting Eq. [3] into Eq. [4] and integrating Eq. [4] leads to

$$Q = \frac{\pi R^4 \gamma_w i}{8\mu} = \frac{R^2 \gamma_w}{8\mu} ia \quad [5]$$

Substituting $Q = K_s iA$ and $a = nA$ into Eq. [5] results in

$$K_s = \frac{nR^2 \gamma_w}{8\mu} \quad [6]$$

where n is the porosity of the soil. In Eq. [6], the key parameter for determining K_s is the representative pore radius R. The weighted average method or the mean value of the associated soil pores were commonly used to represent the pore size R. However, such an average value cannot accurately represent the pore structure of soil, as it neglects the interaction among the pores with different sizes (Leonards, 1962; Garcia-Bengochea et al., 1979). Here, the pore-throat effect is introduced to account for the restriction of liquid water passing from large pores into small pores (Marshall, 1958, 1959). Marshall (1958) proposed an estimation method for the representative pore radius R:

$$R^2 = \frac{n\left[r_1^2 + 3r_2^2 + 5r_3^2 + \ldots + (2m-1)r_m^2\right]}{m^2} \quad [7]$$

where the mean radius of the pores in each of m equal fractions of the total pore space is represented in decreasing order of size by r_1, r_2, r_3, ..., and r_m (cm), respectively. An inherent assumption exists in the derivation of Eq. [7]: all the soil pore sizes have the same probability distribution. However, in real soils, the soil pore distribution exhibits a normal probability function. A new

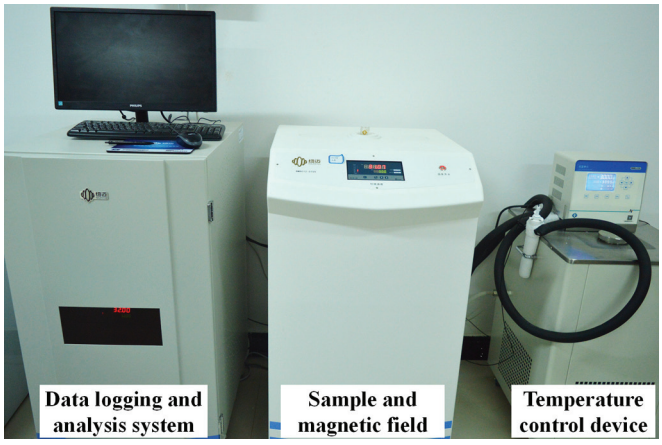

Fig. 1. Photo of the nuclear magnetic resonance (NMR) measurement system.

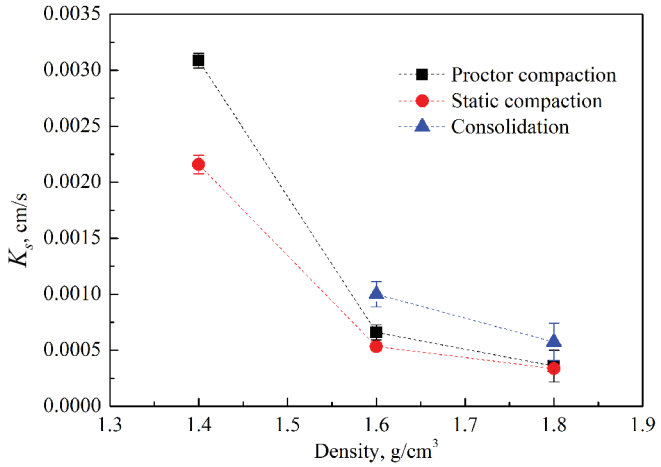

Fig. 2. Schematic diagram of capillary tube model for soil pores. The x axis shows density, and the y axis shows saturated hydraulic conductivity (K_s).

approach should be developed to overcome this inherent assumption in Eq. [7] by considering both the pore-throat effect and soil pore size probability distribution.

The seepage process in a maximal pore of radius r_1 is controlled by the surrounding smaller capillary pores, such that the cross-sectional area for r_1 should be the mean value of all the pore sizes [i.e., $\pi(r_1^2 + r_2^2 + ... + r_m^2)/m$]. For the second largest diameter, r_2, its channel area is limited by pores with smaller diameters. The pore radius of r_2 is also affected by the cross-section of the pore radius r_1. The cross-sectional area related to r_2 can thus be expressed as $\pi(2r_2^2 + ... + r_m^2)/m$, leading to the total cross-sectional area of water volume that must be considered being $\pi[(r_1^2 + r_2^2 + ... + r_m^2) + (2r_2^2 + ... + r_m^2) + ... + mr_m^2]$ or $\pi(r_1^2 + 3r_2^2 + 5r_3^2 + ... + (2m - 1)r_m^2)/m$. Furthermore, the probability distribution function of the pores should be taken into account, since the number of soil pores differ with pore size. The corresponding probabilities for pore sizes $r_1, r_2, ..., r_m$ are expressed as $\omega_1, \omega_2, ..., \omega_m$. The representative pore radius R can then be written as

$$R^2 = \frac{\left[\omega_1 r_1^2 + \omega_2 3r_2^2 + \ldots + \omega_m (2m-1) r_m^2\right]}{m} \quad [8]$$

where ω can be determined according to the pore size distribution curve. Substituting Eq. [8] into Eq. [6] leads to the new method for computing the hydraulic conductivity.

It is noted that a number of expressions have been suggested in the literature for estimating the saturated hydraulic conductivity of soils. Ren et al. (2016) made contrastive analysis for these formulas and proposed a new model for K_s by introducing a new concept of effective void ratio. The result in Ren et al. (2016) shows that the proposed model has reasonable performance for a wide range of soils. The expression is as follows:

$$K_s = C \frac{e_t^{3b+3}}{(1+e_t)^{(5/3)b+1}\left[(1+e_t)^{b+1} - e_t^{b+1}\right]^{4/3}} \quad [9]$$

where b is a positive constant for a given soil; e_t is the total void ratio, which is the summation of the effective void ratio and the ineffective void ratio; and the parameter C is equal to $\gamma_w / C_F \mu \rho_m^2 S_s^2$. Therefore, there are some existing methods that can be used to compare with the new model, including the K–C equation (Eq. [1]), Marshall (1958)'s model (Eq. [6] and [7]), and the model of Ren et al. (2016) (Eq. [9]).

Results and Discussion

Effect of Specimen Preparation on Saturated Hydraulic Conductivity

Figure 3 presents the relationship between K_s and dry density for different specimen preparations. It shows that a greater dry density led to a smaller K_s, irrespective of the sample preparation methods. The value of K_s at the density of 1.4 g cm^{-3} was approximately five to six times greater than K_s at 1.8 g cm^{-3}. The result also indicates that K_s is significantly influenced by the sample preparation method. For a given dry density, such as 1.6 g cm^{-3}, K_s for the consolidated specimen was greater than that for Proctor compaction, whereas static compaction generated the lowest value of K_s. The differences among these three specimen preparation methods can be as large as one order of magnitude, which implies that K_s varies significantly even if the particle size and dry density (void ratio) of the specimens are kept the same. Therefore, it is challenging to determine the hydraulic conductivity accurately using only the information of solid particles. In theory, K_s is related to the pore structure, but the pore information cannot easily be obtained from solid particles.

Figure 4 shows the effect of specimen preparation on pore size distribution under different dry densities. The pore volume ratio is defined as the total volume of soil pores divided by the volume of a certain pore size, which is determined by the signal intensity of the liquid water in a saturated soil specimen by the NMR technology. This figure shows that the specimen prepared by static compaction had very few soil pores >10 μm, unlike the other two preparation methods, leading to lowest saturated hydraulic conductivity. Because the large pores were mainly interaggregate pores, they could provide early flow conduits for the liquid water. Comparing the pore size distribution of the Proctor compaction and consolidated specimens, as shown in Fig. 4b and 4c, the pore size of the consolidated specimen mainly concentrated in the range of 1.6 to 6.3 μm, which presents a more centered pore size distribution. Because the hydraulic process in the maximal pore is controlled by its surrounding smaller capillary pores and the cross-sectional area is controlled by the mean value of all the pore sizes (Marshall, 1958), a more centered pore size distribution indicates a weaker pore throat, leading to a greater hydraulic conductivity.

To verify the new model, the K–C equation and the models proposed by Marshall (1958) and Ren et al. (2016) were used to

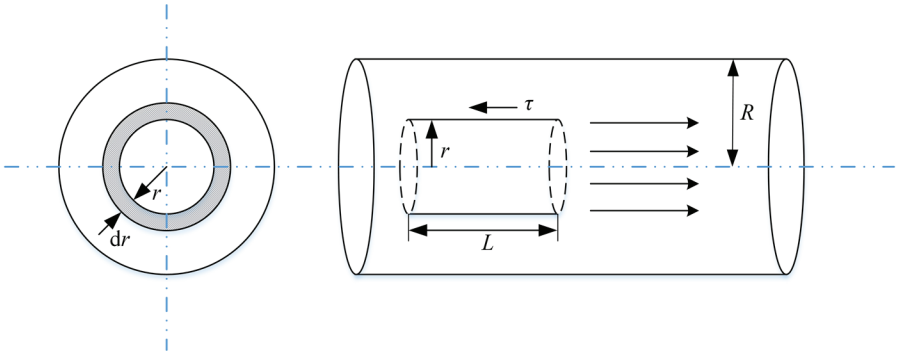

Fig. 3. The saturated hydraulic conductivity vs. dry density for different soil preparation methods. r is the ratio of the tubular water body, L is the length, τ is the water viscosity, and R is the ratio of the capillary tube.

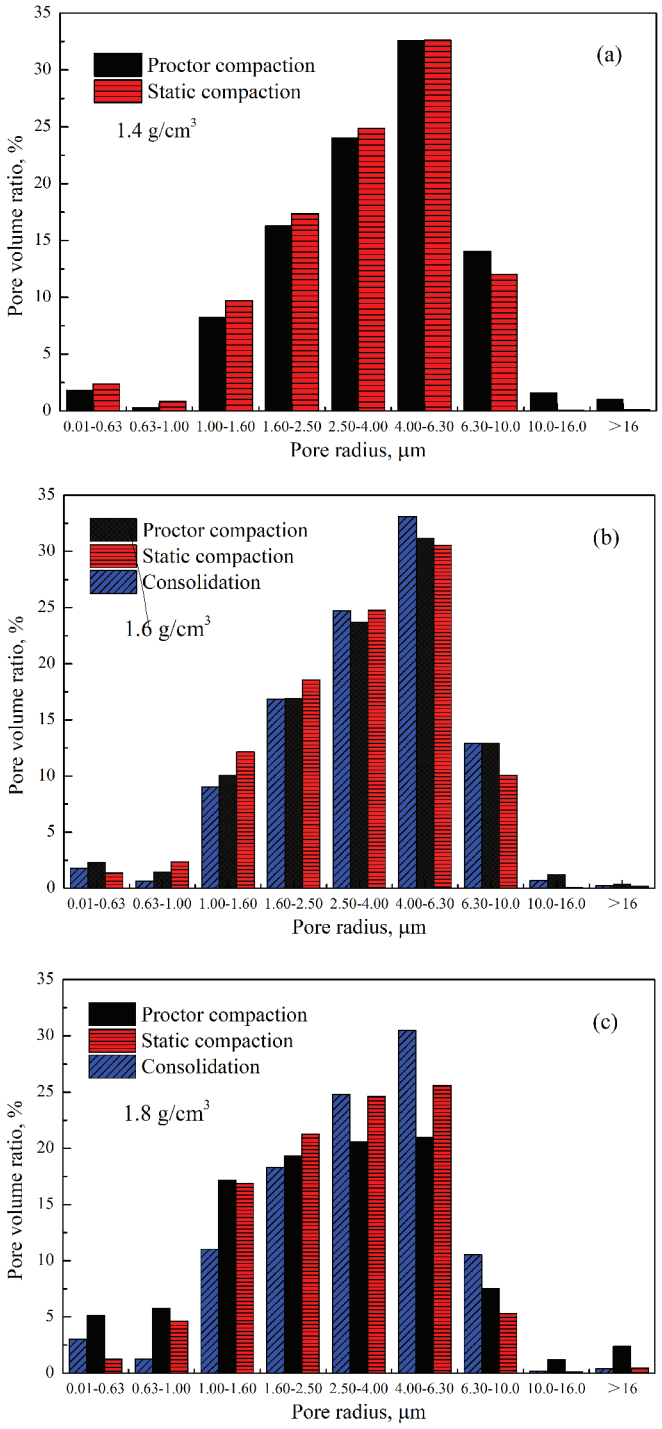

Fig. 4. Pore volume ratio vs. pore radius for different specimen preparations. The dry densities are (a) 1.40, (b) 1.60, and (c) 1.80 g cm^{-3}.

predict the values of K_s. All the predicted results were compared with the measured data. The inputs of these models are summarized in Table 1, and the computed and measured data of K_s are presented in Fig. 5.

It is noted that the K–C equation and Ren et al.'s (2016) model, which are both derived from the void ratio, can only generate a single result for one dry density. Marshall's (1958) model

Table 1. The inputs of the models.†

Models	Density 1.40 g cm^{-3}	Density 1.60 g cm^{-3}	Density 1.80 g cm^{-3}
Kozeny–Carman equation	C_F = 0.20; μ = 1.01; ρ_m = 1.40; S_s = 11.28; e = 0.93; γ_w = 9.80	C_F = 0.20; μ = 1.01; ρ_m = 1.60; S_s = 11.28; e = 0.69; γ_w = 9.80	C_F = 0.20; μ = 1.01; ρ_m = 1.80; S_s = 11.28; e = 0.50; γ_w = 9.80
Ren et al. (2016) model‡	e_t = 0.93; b = 1.10	e_t = 0.69; b = 1.10	e_t = 0.50; b = 1.10
Marshall (1958) model	measured data of the pore size distribution as shown in Fig. 4		
The proposed model	measured data of the pore size distribution as shown in Fig. 4		

† C_F, a dimensionless shape constant; μ, fluid viscosity; ρ_m, soil density; S_s, specific surface area; e, void ratio; γ_w, unit weight of the fluid; b, positive constant for a given soil; e_t, total void ratio.
‡ The values of C_F, μ, ρ_m, S_s, and γ_w in Ren et al. (2016) are the same as that of the Kozeny–Carman equation (Eq. [1]).

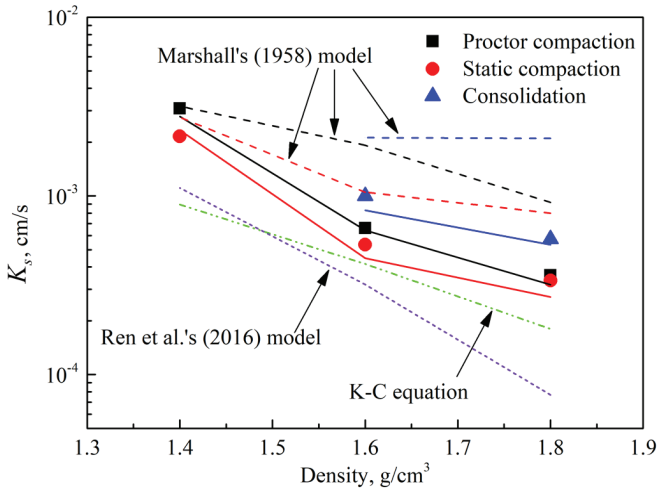

Fig. 5. The comparison between the computed and measured results of saturated hydraulic conductivity (K_s). The solid lines indicate the results predicted by the proposed model: the Marshall (1958) model, the Ren et al. (2016) model, and the Kozeny–Carman (K–C) equation.

(Eq. [6 and 7]) computes K_s based on the soil pore size distribution. It can present three groups of results, as shown by the dashed lines in Fig. 4. The results show the proposed method has a better prediction performance than the other methods. The predictions of the K–C equation and Ren et al. (2016) are quite similar and are always less than the measured data. This is because they do not consider the pore size distribution of soil but use a variable, void ratio, to account for the seepage path. The prediction of Marshall's (1958) model is approximately two to three times greater than the measured values. Compared with the traditional methods in the literature, the proposed model can reveal the essence of seepage flow in soil and generate accurate K_s values. Its cost is that the pore size distribution must be known a priori.

Conclusions

The hydraulic conductivity K_s of soil is usually difficult to measure or predict. The influence of specimen preparations on K_s has rarely been reported. In this study, laboratory tests and theoretical analysis were performed in attempt to gain new understanding of K_s. The following conclusions can be drawn based on the results.

1. Specimen preparation methods have a considerable influence on K_s because they lead to the formation of different pore size distributions. Under the same dry density (or the same porosity), the consolidated specimen tends to have the largest K_s value, followed by those from Proctor compaction and static compaction. The difference among these specimens can be as large as one order of magnitude, indicating that the pore size distribution should be considered in predicting K_s.
2. A pore-information-based theoretical model is presented for estimating K_s, taking into account the interaction between large and small pores and the soil pore size probability distribution. The comparison with the measured data shows that the proposed model is more accurate than traditional void ratio-based models in the literature.

It is noted that the pore size distribution of soil is assumed to be immobile during the permeability test. Further studies should pay attention to the change of soil pore structure when the water is flowing through soil pores. Nevertheless, this study provides new insight into understanding the hydraulic conductivity of soils. The measured results can be used to validate models of hydraulic conductivity.

Acknowledgments

This research was supported by the National Natural Science Foundation of China (No. 51878665, No. 51722812, and No. U1834206), and the Key Research Project supported by the China Railway Corporation (No. K2018G019).

References

Amoozegar, A. 1989. A compact constant-head permeameter for measuring saturated hydraulic conductivity of the vadose zone. Soil Sci. Soc. Am. J. 53:1356–1361. doi:10.2136/sssaj1989.03615995005300050009x

ASTM. 2009. D1557: Standard test methods for laboratory compaction characteristics of soil using modified effort. ASTM Int., West Conshohocken, PA.

ASTM. 2014. D5084-10: Standard test methods for measurement of hydraulic conductivity of saturated porous materials using a flexible wall permeameter. ASTM Int., West Conshohocken, PA.

Bagarello, V., S. Sferlazza, and A. Sgroi. 2009. Testing laboratory methods to determine the anisotropy of saturated hydraulic conductivity in a sandy-loam soil. Geoderma 154:52–58. doi:10.1016/j.geoderma.2009.09.012

Bathke, G.R., and D.K. Cassel. 1991. Anisotropic variation of profile characteristics and saturated hydraulic conductivity in an Ultisol landscape. Soil Sci. Soc. Am. J. 55:333–339. doi:10.2136/sssaj1991.03615995005500020005x

Beckwith, C.W., A.J. Baird, and A.L. Heathwaite. 2003. Anisotropy and depth related heterogeneity of hydraulic conductivity in a bog peat. I: Laboratory measurements. Hydrol. Processes 17:89–101. doi:10.1002/hyp.1116

Bouma, J., and L.W. Dekker. 1981. A method for measuring the vertical and horizontal K_{sat} of clay soils with macropores. Soil Sci. Soc. Am. J. 45:662–663. doi:10.2136/sssaj1981.03615995004500030046x

Boynton, S., and D.E. Daniel. 1985. Hydraulic conductivity tests on compacted clay. J. Geotech. Eng. 111:465–478. doi:10.1061/(ASCE)0733-9410(1985)111:4(465)

Burger, R.L., and K. Belitz. 1997. Measurement of anisotropic hydraulic conductivity in unconsolidated sands: A case study from a shoreface deposit, Oyster, Virginia. Water Resour. Res. doi:10.1029/97WR00570

Carman, P.C. 1937. Fluid flow through a granular bed. Trans. Inst. Chem. Eng. 15:150–156.

Carrier, W.D. 2003. Goodbye Hazen; hello Kozeny–Carman. J. Geotech. Geoenviron. Eng. 129:1054–1056. doi:10.1061/(ASCE)1090-0241(2003)129:11(1054)

Carrier, W.D., and J.F. Beckman. 1984. Correlations between index tests and the properties of remoulded clays. Geotechnique 34:211–228. doi:10.1680/geot.1984.34.2.211

Chapuis, R.P. 2012. Predicting the saturated hydraulic conductivity of soils: A review. Bull. Eng. Geol. Environ. 71:401–434. doi:10.1007/s10064-012-0418-7

Coates, G.R., L.L. Xiao, and M.G. Prammer. 1999. NMR logging principles and application. Halliburton Energy Serv., Houston, TX.

Costa, A. 2006. Permeability-porosity relationship: A reexamination of the Kozeny-Carman equation based on a fractal pore-space geometry assumption. Geophys. Res. Lett. 33:L02318. doi:10.1029/2005GL025134

Delage, P., M. Audiguier, Y.J. Cui, and M.D. Howat. 1996. Microstructure of a compacted silt. Can. Geotech. J. 33:150–158. doi:10.1139/t96-030

Deng, Y.F., A.M. Tang, Y.J. Cui, and X.L. Li. 2011. Study on the hydraulic conductivity of Boom clay. Can. Geotech. J. 48:1461–1470. doi:10.1139/t11-048

Dolinar, B. 2009. Predicting the hydraulic conductivity of saturated clays using plasticity-value correlations. Appl. Clay Sci. 45:90–94. doi:10.1016/j.clay.2009.04.001

Gao, Y., D. Sun, and A. Zhou. 2016. Hydromechanical behaviour of unsaturated soil with different specimen preparations. Can. Geotech. J. 53:909–917. doi:10.1139/cgj-2015-0381

Garcia-Bengochea, I., A.G. Altschaeffl, and C.W. Lovell. 1979. Pore distribution and permeability of silty clays. J. Geotech. Eng. Div. 105:839–856.

Germer, K., and J. Braun. 2015. Determination of anisotropic saturated hydraulic conductivity of a macroporous slope soil. Soil Sci. Soc. Am. J. 79:1528–1536. doi:10.2136/sssaj2015.02.0071

Hillel, D. 1982. Introduction to soil physic. Acad. Press, San Diego, CA. doi:10.2136/sssaj2015.02.0071

Ilek, A., and J. Kucza. 2014. A laboratory method to determine the hydraulic conductivity of mountain forest soils using undisturbed soil samples. J. Hydrol. 519:1649–1659. doi:10.1016/j.jhydrol.2014.09.045

Indraratna, B., V.T. Nguyen, and C. Rujikiatkamjorn. 2012. Hydraulic conductivity of saturated granular soils determined using a constriction-based technique. Can. Geotech. J. 49:607–613. doi:10.1139/t2012-016

Islam, T., and J. Kodikara. 2016. Interpretation of the loading/wetting behaviour of compacted soils within the MPK framework. Part I: Static compaction. Can. Geotech. J. 53:783–805. doi:10.1139/cgj-2014-0316

Iwanek, M. 2008. A method for measuring saturated hydraulic conductivity in anisotropic soils. Soil Sci. Soc. Am. J. 72:1527–1531. doi:10.2136/sssaj2007.0335

Jaeger, F., S. Bowe, H. Vanas, and G.E. Schaumann. 2009. Evaluation of ^{1}H NMR relaxometry for the assessment of pore-size distribution in soil samples. Eur. J. Soil Sci. 60:1052–1064. doi:10.1111/j.1365-2389.2009.01192.x

Jafari, R., V. Sheikh, M. Hossein-Alizadeh, and H. Rezaii-Moghadam. 2017. Effect of soil sample size on saturated soil hydraulic conductivity. Commun. Soil Sci. Plant Anal. 48:908–919. doi:10.1080/00103624.2017.1323086

Jang, J., G.A. Narsilio, and J.C. Santamarina. 2011. Hydraulic conductivity in spatially varying media-a pore-scale investigation. Geophys. J. Int. 184:1167–1179. doi:10.1111/j.1365-246X.2010.04893.x

Kozeny, J. 1927. Uber kapillare Leitung des Wassers im Boden. Sitzungsber. Akad. Wiss. Wien 136:271–306.

Kucza, J., and A. Ilek. 2016. The effect of the shape parameters of a sample on the hydraulic conductivity. J. Hydrol. 534:230–236. doi:10.1016/j.jhydrol.2016.01.010

Leonards, G.A. 1962. Engineering properties of soils. McGraw-Hill Book Co., New York.

Li, X., and L.M. Zhang. 2009. Characterization of dual-structure pore-size distribution of soil. Can. Geotech. J. 46:129–141. doi:10.1139/T08-110

Malusis, M., C.D. Shackelford, and H.W. Olsen. 2003. Flow and transport through clay membrane barriers. Eng. Geol. 70:235–248. doi:10.1016/S0013-7952(03)00092-9

Marshall, T.J. 1958. A relation between permeability and size distribution of pores. Eur. J. Soil Sci. 9:1–8. doi:10.1111/j.1365-2389.1958.tb01892.x

Marshall, T.J. 1959. The diffusion of gases through porous media. Eur. J. Soil Sci. 10:79–82. doi:10.1111/j.1365-2389.1959.tb00667.x

Reeves, A.D., D.E. Henderson, and K.J. Beven. 1996. Flow separation in undisturbed soils using multiple anionic tracers. Part 1. Analytical methods and unsteady rainfall and return flow experiments. Hydrol. Processes 10:1435–1450. doi:10.1002/(SICI)1099-1085(199611)10:11<1435::AID-HYP383>3.0.CO;2-5

Reynolds, W.D. 2008. Saturated hydraulic properties: Laboratory methods. In: M.R. Carter and E.G. Gregorich, editors, Soil sampling and methods of analysis. 2nd ed. CRC Press, Boca Raton, FL. p. 1013–1024.

Reynolds, W.D., and D.E. Elrick. 1985. In situ measurement of field-saturated hydraulic conductivity, sorptivity, and the α-parameter using the Guelph permeameter. Soil Sci. 140:292–302. doi:10.1097/00010694-198510000-00008

Ren, X.W., and J.C. Santamarina. 2018. The hydraulic conductivity of sediments: A pore size perspective. Eng. Geol. 233:48–54. doi:10.1016/j.enggeo.2017.11.022

Ren, X.W., Y. Zhao, Q.L. Deng, J.Y. Kang, D.X. Li, and D.B. Wang. 2016. A relation of hydraulic conductivity: Void ratio for soils based on Kozeny-Carman equation. Eng. Geol. 213:89–97. doi:10.1016/j.enggeo.2016.08.017

Sheng, D., S. Zhang, F. Niu, and G. Cheng. 2014. A potential new frost heave mechanism in high-speed railway embankments. Géotechnique 64:144–154. doi:10.1680/geot.13.P.042

Surridge, B.W., A.J. Baird, and A.L. Heathwaite. 2005. Evaluating the quality of hydraulic conductivity estimates from piezometer slug tests in peat. Hydrol. Processes 19:1227–1244. doi:10.1002/hyp.5653

Tarantino, A. 2011. Unsaturated soils: Compacted versus reconstituted states. In: E.E. Alonso and A. Gens, editors, Unsaturated soils. CRC Press, Barcelona, Spain. p. 113–136.

Tarantino, A., and E. de Col. 2008. Compaction behaviour of clay. Geotechnique 58:199–213. doi:10.1680/geot.2008.58.3.199

Taylor, D.W. 1948. Fundamentals of soil mechanics. John Wiley & Sons, New York.

Teng, J., F. Shan, Z. He, S. Zhang, and D. Sheng. 2019a. Experimental study of ice accumulation in unsaturated clean sand. Geotechnique 69:251–259. doi:10.1680/jgeot.17.P.208

Teng, J., N. Yasufuku, Q. Liu, and S. Liu. 2014. Experimental evaluation and parameterization of evaporation from soil surface. Nat. Hazards 73:1405–1418. doi:10.1007/s11069-014-1138-z

Teng, J., N. Yasufuku, S. Zhang, and Y. He. 2016. Modelling water content redistribution during evaporation from sandy soil in presence of water table. Comput. Geotech. 75:210–224. doi:10.1016/j.compgeo.2016.02.009

Teng, J., X. Zhang, S. Zhang, C. Zhao, and D. Sheng. 2019b. An analytical model for evaporation from unsaturated soil. Comput. Geotech. 108:107–116. doi:10.1016/j.compgeo.2018.12.005

Venkatarama Reddy, B.V., and K.S. Jagadish. 1993. The static compaction of soils. Geotechnique 43:337–341. doi:10.1680/geot.1993.43.2.337

Wyllie, M.R.J., A.R. Gregory, and G.H.F. Gardner. 1958. An experimental investigation of factors affecting elastic wave velocities in porous media. Geophysics 23:459–493. doi:10.1190/1.1438493

Zhang, S., J. Teng, Z. He, Y. Liu, S. Liang, Y. Yao, and D. Sheng. 2016. Canopy effect caused by vapour transfer in covered freezing soils. Geotechnique 66:927–940. doi:10.1680/jgeot.16.P.016